

Article

Using Sentinel-2 Data for Retrieving LAI and Leaf and Canopy Chlorophyll Content of a Potato Crop

Jan G. P. W. Clevers ^{1,*}, Lammert Kooistra ¹ and Marnix M. M. van den Brande ^{2,†}

¹ Laboratory of Geo-Information Science and Remote Sensing, Wageningen University & Research, P.O. Box 47, 6700 AA Wageningen, The Netherlands; lammert.kooistra@wur.nl

² Van den Borne Aardappelen, Postelsedijk 15, 5541 NM Reusel, The Netherlands; marnix.vandenbrande@gmail.com

* Correspondence: jan.clevers@wur.nl; Tel.: +31-317-481-802

† Present address: Water Board Scheldestromen, P.O. Box 1000, 4330 ZW Middelburg, The Netherlands.

Academic Editors: Jose Moreno and Prasad S. Thenkabail

Received: 29 March 2017; Accepted: 13 April 2017; Published: 25 April 2017

Abstract: Leaf area index (LAI) and chlorophyll content, at leaf and canopy level, are important variables for agricultural applications because of their crucial role in photosynthesis and in plant functioning. The goal of this study was to test the hypothesis that LAI, leaf chlorophyll content (LCC), and canopy chlorophyll content (CCC) of a potato crop can be estimated by vegetation indices for the first time using Sentinel-2 satellite images. In 2016 ten plots of 30 × 30 m were designed in a potato field with different fertilization levels. During the growing season approximately 10 daily radiometric field measurements were used to determine LAI, LCC, and CCC. These radiometric determinations were extensively calibrated against LAI2000 and chlorophyll meter (SPAD, soil plant analysis development) measurements for potato crops grown in the years 2010–2014. Results for Sentinel-2 showed that the weighted difference vegetation index (WDVI) using bands at 10 m spatial resolution can be used for estimating the LAI (R^2 of 0.809; root mean square error of prediction (RMSEP) of 0.36). The ratio of the transformed chlorophyll in reflectance index and the optimized soil-adjusted vegetation index (TCARI/OSAVI) showed to be a good linear estimator of LCC at 20 m (R^2 of 0.696; RMSEP of 0.062 $\text{g}\cdot\text{m}^{-2}$). The performance of the chlorophyll vegetation index (CVI) at 10 m spatial resolution was slightly worse (R^2 of 0.656; RMSEP of 0.066 $\text{g}\cdot\text{m}^{-2}$) compared to TCARI/OSAVI. Finally, results showed that the green chlorophyll index (CI_{green}) was an accurate and linear estimator of CCC at 10 m (R^2 of 0.818; RMSEP of 0.29 $\text{g}\cdot\text{m}^{-2}$). Results for CI_{green} were better than for the red-edge chlorophyll index ($\text{CI}_{\text{red-edge}}$, R^2 of 0.576, RMSE of 0.43 $\text{g}\cdot\text{m}^{-2}$). Our results show that Sentinel-2 bands at 10 m spatial resolution are suitable for estimating LAI, LCC, and CCC, avoiding the need for red-edge bands that are only available at 20 m. This is an important finding for applying Sentinel-2 data in precision agriculture.

Keywords: Sentinel-2; potato canopy; leaf area index; leaf chlorophyll content; canopy chlorophyll content; vegetation indices

1. Introduction

Foliar biochemistry (in particular chlorophyll content) is a key proxy of plant productivity and plays a crucial role in photosynthesis and in plant functioning [1]. Remote sensing data can provide location-specific information of chlorophyll content as a proxy of the crop nitrogen (N) status in order to help farmers with an optimal in-season timing of N application (side dress) [2,3]. It can provide the spatial information needed for the implementation of variable rate application (VRA) in order to optimize production across an entire field. For precision agriculture the spatial resolution should be at least 20 m and, preferably, on the order of 10 m in order to make site specific management

possible [4]. The revisit time should only be a few days. Freely-available data from Sentinel-2 seems to fulfil these requirements.

Optical remote sensing techniques respond mainly to vegetation characteristics, like the leaf area index (LAI) and the chlorophyll content, particularly providing information at the canopy scale. For this purpose several remote sensing techniques have been proposed, either based on radiative transfer (RT) model inversion or (semi-)empirical spectral vegetation indices [5]. Hybrid approaches integrate a sensitivity analysis using RT models with the practical use of vegetation indices (VI) [6]. In this study, we will focus on using VIs. A semi-empirical approach for estimating LAI of a green canopy, introduced by Clevers [7], resulted in the so-called weighted difference vegetation index (WDVI). Basically, the WDVI is a two-dimensional greenness index. This index can be easily obtained with field radiometric measurements and can be used for estimating LAI as a replacement for destructive measurements [8]. The canopy chlorophyll content (CCC) is determined by the LAI and the leaf chlorophyll content (LCC), expressed per unit leaf area. Estimating LCC requires a VI that is sensitive to this LCC but, at the same time, is insensitive to LAI and background effects. Kooistra and Clevers [9] showed that two ratio indices have great potential to be applied using Sentinel-2 data. The ratio of the transformed chlorophyll in reflectance index and the optimized soil-adjusted vegetation index (TCARI/OSAVI) is one index following the idea of the above ratio approach for estimating LCC [10]. In addition, Vincini et al. [11] proposed the green/red ratio to normalize the LAI, resulting in the so-called chlorophyll vegetation index (CVI) as an estimator for LCC. For estimating CCC the red-edge region is also found to be very important. Gitelson et al. [12] presented a simple index based on a near-infrared and a red-edge band for estimating CCC, called the red-edge chlorophyll index ($CI_{red-edge}$). They also presented a version using a green band instead of the red-edge band, called the green chlorophyll index (CI_{green}). Both indices can be evaluated using Sentinel-2 data [13].

This study should provide a proof of concept of using real Sentinel-2 spectral data in estimating LAI, LCC, and CCC for applications in precision agriculture. Previous results showed that the WDVI may be used for estimating the LAI. Either the TCARI/OSAVI or the CVI may be applied in estimating the LCC. Subsequently, for estimating the CCC, the $CI_{red-edge}$ and the CI_{green} indices are very promising in combination with Sentinel-2 data. The main objective of the current study is to test the performance of these indices using actual Sentinel-2 data over the 2016 growing season for a potato crop, being one of the most important cash crops in Western Europe.

2. Material and Methods

2.1. Study Site

The study area was a field with potatoes (*Solanum tuberosum* L., cultivar Fontane) of approximately 450 m × 200 m, located south of the village Reusel (51°59'47.9"N, 5°9'34.5"E) on the Dutch–Belgian border, in the province of Noord-Brabant (The Netherlands). The planting date was 16 April 2016. In this field, an experiment was performed to evaluate the effect of split-level fertilization on potato yield. Different initial fertilization levels (before planting) and additional sensor-based variable-rate fertilizations (during crop growth) were applied to zones in the field. The sensor-based variable-rate fertilization was applied based on crop reflectance measurements performed by Isaria crop sensors (Fritzmeier Umwelttechnik GmbH & Co., KG, Grosshelfendorf, Germany) mounted in front of a tractor providing information on the nitrogen need of the crop on a weekly basis. The variable rates for nitrogen were based on measured indices from the crop sensor and decision rules derived from previous dedicated fertilization experiments between 2010 and 2013 [14], and applied using a GNSS-guided fertilizer spreader. Ten 30 m × 30 m net plots were created in the different fertilization zones (Figure 1 and Table 1). Sensor-based nitrogen (N) fertilization was applied to half of the plots on 28 June 2016, 15 July 2016, and 9 August 2016. In addition, on 7 July 2016 fertilization with potassium (K) was applied to most of the plots. These varying fertilization regimes were expected to yield significant differences in crop development.

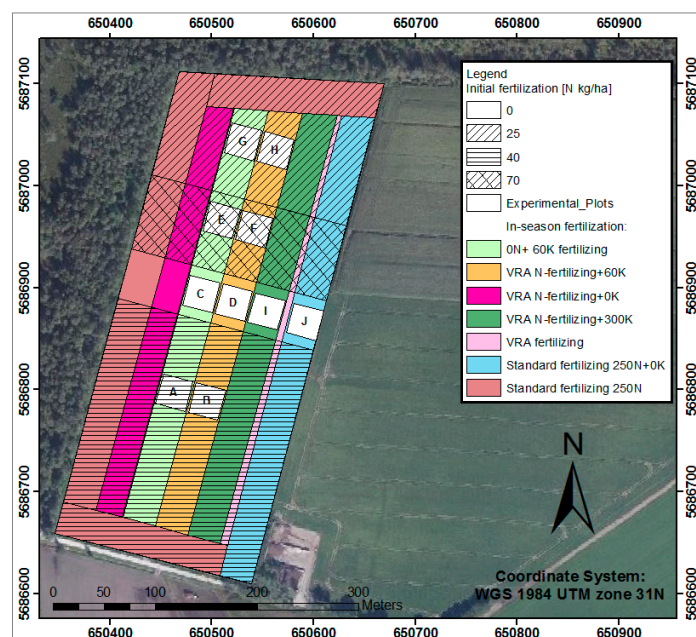


Figure 1. The study area with the 2016 potato field showing the zones with initial fertilization levels, the zones with variable rate applications (VRA), and the location of the studied plots. An aerial photograph is used as the background.

Table 1. An overview of the nitrogen (N) and potassium (K) fertilization applied to the various plots within the potato experimental field in 2016.

Plot	Initial Fertilization (N kg·ha ⁻¹)	28 June (N kg·ha ⁻¹)	7 July (K kg·ha ⁻¹)	15 July (N kg·ha ⁻¹)	9 August (N kg·ha ⁻¹)
A	40	0	60	0	0
B	40	42	60	30	45
C	0	0	60	0	0
D	0	140	60	30	34
E	70	0	60	0	0
F	70	0	60	49	47
G	25	0	100	0	0
H	25	84	60	38	28
I	0	0	300	50	27
J	0	269	0	30	26

2.2. Field Radiometry

Field methods for determining canopy properties, like LAI and chlorophyll content, are mostly destructive, expensive, and time-consuming. As a result, they are mostly performed for relatively small crop samples. Radiometric field measurements are non-invasive and can be performed over much larger areas, providing a more accurate areal estimate. After proper calibration, such measurements are a good alternative for destructive measurements, as shown by Bouman et al. [8] for crops like potato, sugar beet, wheat, and barley. They used the WDVI (Table 2) [7] measured with a CropScan multispectral radiometer (MSR87, CropScan Inc., Rochester, MN, USA), which has been shown to work very well for estimating ground cover and LAI of the mentioned crops using standard relations that are crop type-specific [8]. Nowadays, such measurements are, for instance, being used for a reflectance-based N side dress system for potatoes that allows saving of N while maintaining yield [2]. Radiometric measurement of crop N status offers advantages over destructive methods. It is quick, cheap, and can be done on every square meter of a field.

Recent work by Kooistra and Clevers [9] has shown that other vegetation indices may be used to estimate leaf chlorophyll content (LCC). They found that the TCARI/OSAVI ratio and the CVI are the most promising as LCC estimators (Table 2). Subsequently, the product of the estimated LAI and LCC from radiometric measurements will provide the canopy chlorophyll content (CCC). However, since errors in the estimates of LAI and LCC will accumulate in this way, it is preferred to use specific indices for estimating CCC, like the $CI_{red-edge}$ and the CI_{green} [6,13].

Table 2. Vegetation indices evaluated in this study.

Index	Formulation	Reference
WDVI	$R_{870} - C \times R_{670}$ with $C = \frac{R_{870,soil}}{R_{670,soil}}$	[7]
TCARI/OSAVI	$\frac{3[(R_{700} - R_{670}) - 0.2(R_{700} - R_{550})(R_{700}/R_{670})]}{(1 + 0.16)(R_{800} - R_{670})/(R_{800} + R_{670} + 0.16)}$	[10]
CVI	$\frac{R_{870}}{R_{550}} \times \frac{R_{670}}{R_{550}}$ or $\frac{R_{870}/R_{550}}{R_{550}/R_{670}}$	[11]
$CI_{red-edge}$	$\frac{R_{780}}{R_{705}} - 1$	[12]
CI_{green}	$\frac{R_{780}}{R_{550}} - 1$	[12]

R_x refers to the reflectance at wavelength x nm.

Vegetation reflectance for the experimental plots given in Table 1 was measured about every 10 days in the period from 4 June 2016 until 19 August 2016 with a Cropscan Multispectral Radiometer (MSR16R). This is a 16-band radiometer measuring reflected and incoming radiation at the same moment in narrow spectral bands (Table 3). Reflectance is measured through a 28° field-of-view (FOV) aperture at a height of about 1.5 m above the canopy and incoming radiation is measured through a cosine-corrected sphere. As a result, the area of individual measurements covered about 0.44 m². Calibration is performed by pointing the 28° FOV aperture towards the sun using an opal glass. Using this calibration, spectral reflectances are derived.

The ground-based apparent LAI was estimated based on Cropscan measurements using the WDVI with bands at 670 nm and 870 nm [7]. Calibration curves between the WDVI and LAI were determined by performing both Cropscan measurements and LAI2000 Plant Canopy Analyser (LI-COR, Lincoln, NE, USA) measurements in the field at the same farm for potato experiments with similar set-ups in the years 2010–2014 [9]. Per plot, six measurements per potato row, for four rows (24 values per plot), were taken. The 2000–2014 experiments resulted in the following relationship:

$$LAI = 0.109 \times WDVI - 0.3233 \quad (1)$$

For potatoes grown in the years 2010–2014 LCC was measured per plant, taking the average reading of three randomly-selected leaves using a hand-held chlorophyll meter (SPAD-502, Minolta Osaka Company Ltd., Tokyo, Japan). SPAD measurements were converted to LCC using the potato-specific relationship given by Uddling et al. [15]. The 2000–2014 experiments resulted in the following relationship for TCARI/OSAVI (using the Cropscan bands at 550, 670, 700, and 780 nm) with LCC (in g·m⁻²):

$$LCC = -3.5884 \times TCARI/OSAVI + 1.0369 \quad (2)$$

Finally, CCC was estimated by the $CI_{red-edge}$ using the Cropscan bands at 780 nm and 705 nm (as the average reflectance of 700 and 710 nm):

$$CCC = 0.8013 \times CI_{red-edge} - 0.4704 \quad (3)$$

Based on the quality of the established relations as assessed through an independent validation with available field measurements in 2016 (LAI: RMSE = 0.57; LCC: RMSE = 0.10 $\text{g}\cdot\text{m}^{-2}$; CCC: RMSE = 0.69 $\text{g}\cdot\text{m}^{-2}$), we have confidence in the Cropscan-derived crop variables.

Table 3. Specifications of the Cropscan MSR16R system.

Center Wavelength (nm)	Band Width (nm)
490	7.3
530	8.5
550	9.2
570	9.7
670	11
700	12
710	12
740	13
750	13
780	11
870	12
940	13
950	13
1000	15
1050	15
1650	200

2.3. Sentinel-2

ESA launched the first Sentinel-2 (called 2A) polar-orbiting satellite in June 2015. It carries the Multi-Spectral Instrument (MSI), having four bands at 10 m, six bands at 20 m, and three bands at 60 m spatial resolution. The latter are dedicated to atmospheric corrections and cloud screening [16]. It has a swath width of 290 km by applying a total field-of-view of about 20°. It covers the visible and near-infrared (NIR) and the shortwave-infrared (SWIR) spectral region, incorporating two spectral bands in the so-called red-edge region, which are important for the retrieval of chlorophyll content [17–19]. These red-edge bands are centered at 705 and 740 nm with a band width of 15 nm and a spatial resolution of 20 m (Table 4). Table 5 provides an overview of the Sentinel-2 images available for the study site during the growing season of 2016. These images were atmospherically corrected using the SEN2COR procedure available in the Sentinel-2 SNAP (Sentinel Application Platform) toolbox, converting top-of-atmosphere (TOA) reflectances into top-of-canopy (TOC) reflectances [20]. SEN2COR performs a pre-processing of TOA image data and applies a scene classification for atmospheric correction. The latter focuses on the detection of snow, clouds, and cloud shadows, as opposed to the broad classes of vegetation, bare soil, and water. Atmospheric bands of Sentinel-2 are used to derive maps of aerosols, water vapor and cirrus clouds [20]. Atmospheric correction is based on the ATCOR algorithm [21]. For most dates the study area and its surroundings was cloud-free. Only on 10 July 2016 were there scattered clouds across the region. The experimental field was cloud-free, but there was a cloud visible to the west of the field and a cloud shadow to the east of the field. This may cause atmospheric correction to be less accurate for this date. TOC products were the result of a resampling procedure with a constant ground resampling distance of 10 m or 20 m depending on the native resolution (Table 4) using a digital elevation model to project images in cartographic coordinates (UTM/WGS84 projection). For each available date plot reflectances were obtained by extracting the 20 m pixel that best covered the net plots (being at least within the gross plots, thus avoiding problems with mixed pixels). A polygon with field boundaries was used to check the geometric co-registration. Average geometric inaccuracies were less than 10 m. For some images a pixel shift of one pixel had to be applied (avoiding a further averaging of pixels). In the case of 10 m spectral bands, the four pixels within a 20 m pixel were averaged.

Table 4. Specifications of the Multi-Spectral Instrument (MSI) on the Sentinel-2 satellite system.

Spectral Band	Center Wavelength (nm)	Band Width (nm)	Spatial Resolution (m)
B1	443	20	60
B2	490	65	10
B3	560	35	10
B4	665	30	10
B5	705	15	20
B6	740	15	20
B7	783	20	20
B8	842	115	10
B8a	865	20	20
B9	945	20	60
B10	1380	30	60
B11	1610	90	20
B12	2190	180	20

Table 5. Specifications of Sentinel-2 overflights over the test site during the growing season of 2016.

Date	Orbit	Solar Zenith Angle (°)	Solar Azimuth Angle (°)	View Zenith Angle (°)	View Azimuth Angle (°)
8 May 2016	8	35.44	159.56	8.00	99.98
7 June 2016	8	30.22	155.94	8.04	99.99
10 July 2016	51	30.65	157.81	5.61	279.37
20 July 2016	51	32.27	158.19	5.63	279.41
16 August 2016	8	39.52	158.02	8.01	99.96
26 August 2016	8	42.64	160.08	8.00	99.96
8 September 2016	51	46.66	166.20	5.65	279.41
25 September 2016	8	53.29	166.18	8.11	99.99
5 October 2016	8	57.01	167.82	8.11	99.99

For estimating the LAI, Sentinel-2 TOC spectral values were used to calculate the WDVI. The bands B8 (842 nm) and B4 (665 nm) provide estimates at 10 m spatial resolution. Based on images early in the year (8 May 2016) with bare soil, the slope of the soil line (C parameter in Table 2) was estimated as 1.35 for these spectral bands.

For estimating the LCC, first the TCARI/OSAVI was tested, using TOC values of Sentinel-2 bands B3 (560 nm), B4 (665 nm), B5 (705 nm), and B7 (783 nm). Since bands B5 and B7 are only available at 20 m spatial resolution, the final LCC estimate will also be only available at 20 m. In addition, the CVI was also tested using bands B3, B4, and B8, which are all using a spatial resolution of 10 m, as previous research has shown that this index is also very promising [9].

For estimating the CCC, both the $CI_{red-edge}$ and the CI_{green} were tested. The second one is also interesting using Sentinel-2, since it avoids the need for red-edge bands that are only available at 20 m [13]. $CI_{red-edge}$ was calculated using Sentinel-2 TOC values in bands B7 (783 nm) and B5 (705 nm), both at 20 m spatial resolution. The CI_{green} was calculated using bands B8 (842 nm) and B3 (560 nm) that both have a spatial resolution of 10 m.

Calibration curves obtained for the Cropscan system cannot be directly applied to the Sentinel-2 data, because band positions and, particularly, band widths are mostly quite different (Tables 3 and 4). This difference adds to the difference in scale level, the measurement area, and the measurement conditions (sometimes there is a few days' difference between Cropscan and Sentinel-2 observations). Therefore, new empirical relationships were ascertained between the derived vegetation indices based on the Sentinel-2 images and the crop variables LAI, LCC, and CCC. The coefficient of determination (R^2) was used as a measure of scatter around the regression line. Due to the limited number of observations for such re-parameterizations (40 observations) validation was performed using the

leave-one-out procedure. The root mean square error of prediction (RMSEP) was adopted to evaluate the established relations and the goodness of fit.

3. Results and Discussion

3.1. Sentinel-2 Temporal Profiles

First, the quality of the Sentinel-2 reflectances was evaluated. Figure 2a illustrates the difference between the TOA and TOC reflectances for an example plot. The difference is caused by the SEN2COR atmospheric correction procedure. We chose an example plot from 10 July 2016 since atmospheric conditions were suboptimal due to scattered small clouds in the vicinity of the study site. As usual, in the visible part of the spectrum, TOA reflectances are higher compared to TOC reflectances due to the significant contribution of atmospheric path radiance, particularly in the blue portion of the spectrum. As a result, the typical peak in green reflectance is not pronounced in the TOA reflectance spectrum. In the NIR and SWIR this path radiance is very small and atmospheric attenuation causes lower values for the TOA reflectance in comparison to the TOC reflectance. When we compare the TOC reflectance signature with the one measured in the field with the Cropscan radiometer, we find very similar signatures (Figure 2b). Similar good results were obtained for other plots and other dates (not shown). Field measurements of crop variables and the Cropscan were performed until mid-August, because after that date measurements are less relevant for farmers in view of applying precision agriculture. As a result, data for four dates in 2016 (7 June, 10 July, 20 July, and 16 August) are available for studying the relationship of Sentinel-2 TOC reflectances and indices with crop variables. Comparing the TOC reflectances with the Cropscan reflectances showed very good correlations when combining these four dates for all potato plots.

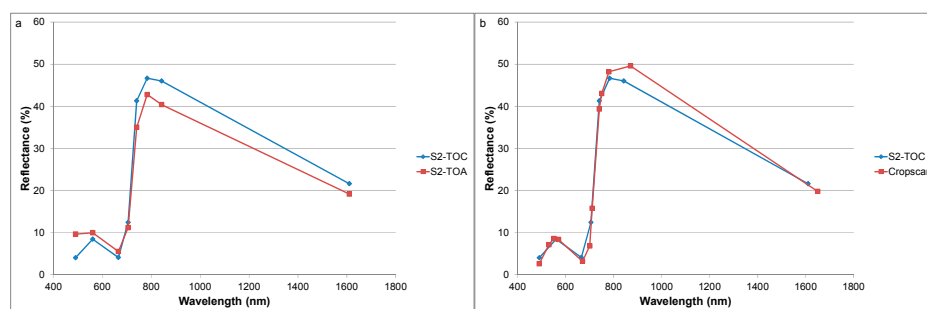


Figure 2. Illustration of the comparison between (a) the TOA reflectance and the TOC reflectance for Sentinel-2, and (b) the TOC reflectance signature for Sentinel-2 and for the Cropscan. The example shows plot A of the potato experimental field, 10 July 2016.

Subsequently, the temporal pattern of WDVI, as an estimator for the LAI, is illustrated in Figure 3. At the beginning of May the WDVI was still close to zero, since there was no vegetation development yet. The WDVI then increased during June with plants standing upright above the ridges, still showing a clear row structure. Flowering occurred around the maximum LAI, which took place at the beginning of July 2016. Subsequently, the WDVI decreased gradually towards the end of the season. Although it is not the objective of this paper to discuss all plots individually and all differences amongst them, we clearly noticed, for most dates, that the lowest WDVI value was for plot C, which received no N fertilization at all. From mid-July, onwards, plot G also had a relatively low WDVI. This plot received the second-lowest level of initial N fertilization, and no N fertilization during the season.

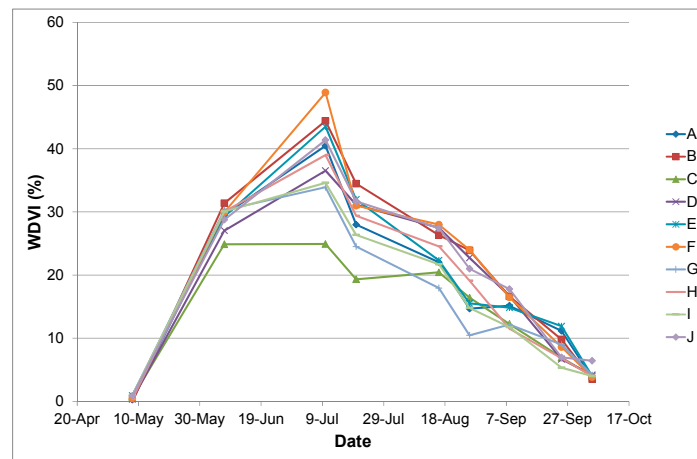


Figure 3. Temporal profiles of the WDV index obtained from Sentinel-2 at 10 m resolution for the ten potato plots of the test area in 2016.

Figure 4 illustrates the temporal profiles for TCARI/OSAVI and CVI, which are hypothesized to be related to the LCC. The TCARI/OSAVI mainly showed differences between the plots at the beginning and the end of the growing season, which might also be caused by differences between plots in the soil background effect instead of differences in the LCC. For most of the season, differences were rather small. Moreover, this index was rather stable over the season, suggesting a small range in the LCC for this potato crop. The LCC was not correlated with LAI ($R^2 = 0.062$). The CVI showed even less differences between the plots. The second recording date (7 June 2016) clearly showed larger CVI values than for most of the season. Since the beginning of July plot J was showing relatively high CVI values. This is the plot that received a large burst of N at the end of June 2016 (Table 1). The advantage of the CVI is that it can be determined at 10 m with Sentinel-2, whereas the TCARI/OSAVI ratio can only be determined at 20 m.

Finally, Figure 5 illustrates the temporal profiles for $CI_{red-edge}$ and CI_{green} , which are both often used to estimate the CCC. The $CI_{red-edge}$ showed a similar pattern as the WDV. This is not so surprising, because we saw before that variation in the LCC was not very large and, thus, the LAI was mainly determining the CCC. Figure 5a underlines this hypothesis. The same patterns can be observed for the CI_{green} , although there was not such a pronounced peak in CI_{green} at the beginning of July. The advantage of the CI_{green} is that it can be determined at 10 m with Sentinel-2, whereas the $CI_{red-edge}$ can only be determined at 20 m due to the use of the red-edge bands.

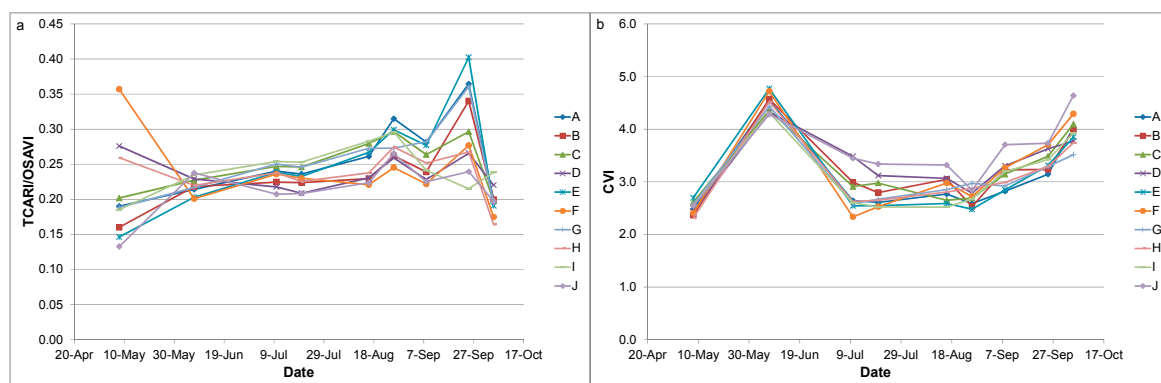


Figure 4. Temporal profiles of the TCARI/OSAVI (a) and the CVI (b) obtained from Sentinel-2 for the ten potato plots of the test area in 2016.

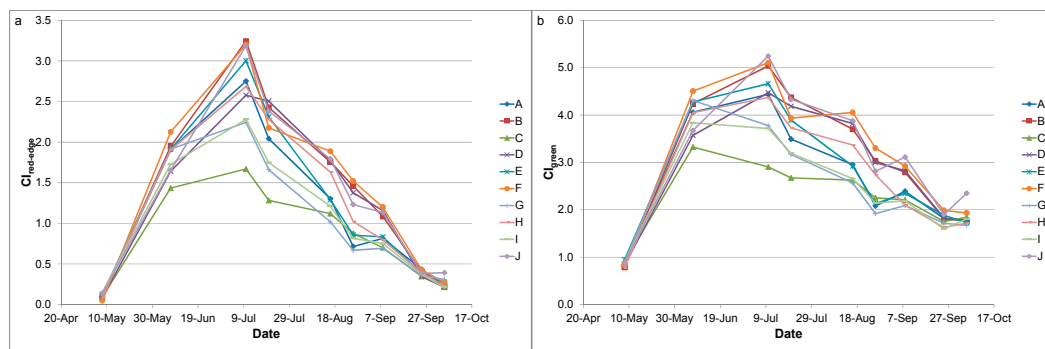


Figure 5. Temporal profiles of the $CI_{red-edge}$ (a) and CI_{green} (b) obtained from Sentinel-2 for the ten potato plots of the test area in 2016.

3.2. LAI Estimation

Sentinel-2 TOC results confirmed the existence of a good relationship between the WDV and the apparent LAI, as derived from radiometric (Cropscan) field measurements (Table 6). Combining the four dates yielded a significant linear relationship between WDV and LAI with an R^2 of 0.809 (Figure 6a). All R^2 values were significant at the 5% confidence level. Applying a leave-one-out cross-validation procedure on the linear relationship yielded a root mean square error of prediction (RMSEP) of 0.36 (equals 10.1% of the mean LAI). The relationship between the measured LAI (using the Cropscan) and the estimated LAI using Sentinel-2 is illustrated in Figure 6b.

Table 6. Coefficients of determination (R^2) between the studied vegetation indices and crop variables for Sentinel-2 overflights over the test site during the growing season of 2016.

Date	WDV-LAI	TCARI/OSAVI-LCCCVI-LCC	$CI_{red-edge}$ -CCC	CI_{green} -CCC
7 June 2016	0.708	0.501	0.412	0.903
10 July 2016	0.920	0.668	0.816	0.778
20 July 2016	0.875	0.650	0.636	0.845
16 August 2016	0.916	0.742	0.711	0.932
4 dates combined	0.809	0.696	0.656	0.818

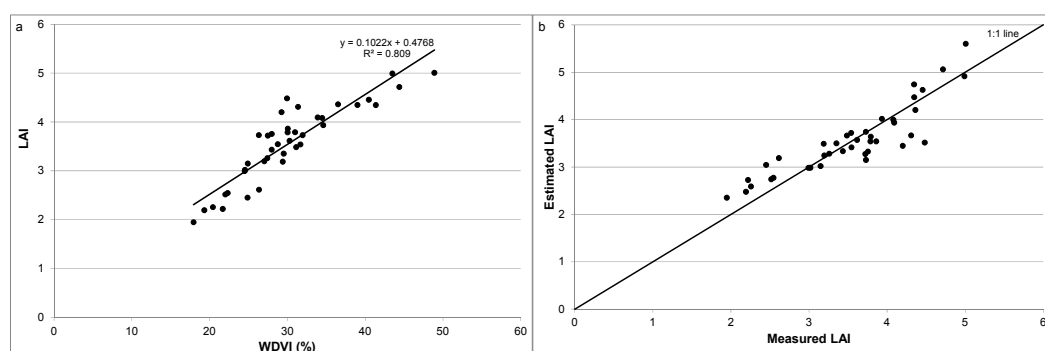


Figure 6. The relationship between the WDV and the apparent LAI (a) and between measured and estimated LAI (b) for the ten plots of the potato experiment on 4 dates in 2016 using Sentinel-2 data at 10 m resolution.

3.3. LCC Estimation

Table 6 shows that there are reasonable relationships with the LCC of both the TCARI/OSAVI index and the CVI index based on Sentinel-2 TOC data for the ten potato plots of the study site. Only for the first date, when the canopy cover, on average, was still around 60%, results were somewhat worse

(Table 6, line for 7 June 2016). All R^2 values were significant at the 5% confidence level. Combining the four dates yielded a significant linear relationship between TCARI/OSAVI and LCC with an R^2 of 0.696 (Figure 7a). This index can be calculated at 20 m spatial resolution using Sentinel-2. Applying a leave-one-out cross-validation procedure on the linear relationship yielded an RMSEP of $0.062 \text{ g}\cdot\text{m}^{-2}$ (12.3% of the mean LCC). The relationship between the measured LCC (using the Cropscan) and the estimated LCC using Sentinel-2 is illustrated in Figure 7b.

The CVI can be calculated at 10 m spatial resolution with Sentinel-2 data. The problem may be that it uses the square of the reflectance in the green band in the denominator and the red reflectance in the nominator. Since both green and red reflectances of vegetation are rather small numbers, the accuracy of such values is critical in a ratio-type index. Figure 8a confirmed such problems in calculating the relationship between the CVI and LCC. Particularly, the fourth date (16 August 2016) showed some deviating low LCC values. Still, the linear relationship was highly significant with an R^2 of 0.656 and an RMSEP of $0.066 \text{ g}\cdot\text{m}^{-2}$ (13.0%). Figure 8b illustrates the scatterplot of estimated against measured LCC using the CVI.

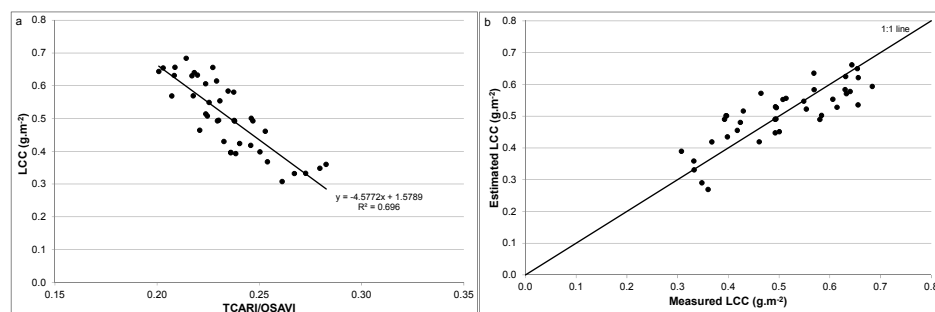


Figure 7. The relationship between the TCARI/OSAVI index and the LCC (a) and between measured and estimated LCC (b) for the ten plots of the potato experiment on four dates in 2016 using Sentinel-2 data at 20 m resolution.

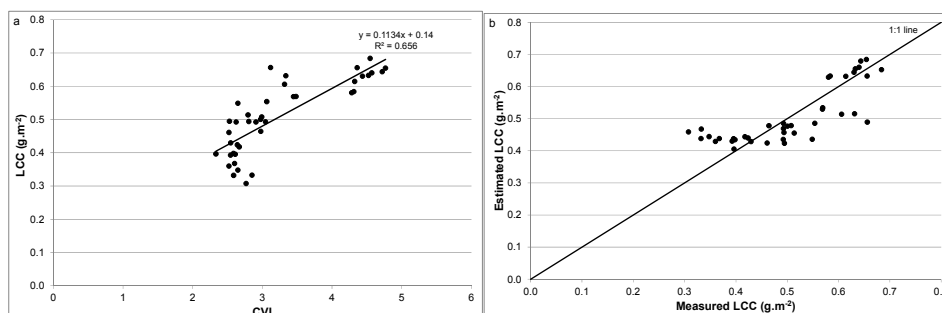


Figure 8. The relationship between the CVI index and the LCC (a) and between measured and estimated LCC (b) for the ten plots of the potato experiment on four dates in 2016 using Sentinel-2 data at 10 m resolution.

3.4. CCC Estimation

We expect significant linear relationships of both $CI_{\text{red-edge}}$ and CI_{green} with the CCC. Table 6 shows that this is, indeed, true for the four dates individually. For some dates the $CI_{\text{red-edge}}$ performed better, whereas on other dates the CI_{green} performed better. On average, their performance was similar and all R^2 values were significant at the 5% confidence level. The main difference for practical applications is that the $CI_{\text{red-edge}}$ can only be determined at 20 m resolution with Sentinel-2 data, whereas the CI_{green} can be determined at 10 m. Combining the four dates yielded a significant linear relationship between $CI_{\text{red-edge}}$ and CCC with an R^2 of 0.576 (Figure 9a). Applying a leave-one-out cross-validation procedure on the linear relationship yielded an RMSEP of $0.43 \text{ g}\cdot\text{m}^{-2}$ (22.9% of the

mean CCC). The relationship between the measured CCC (using the Cropscan) and the estimated CCC using Sentinel-2 is illustrated in Figure 9b.

Figure 10a shows a significant linear relationship between CI_{green} and CCC with an R^2 of 0.818 and an RMSEP of $0.29 \text{ g}\cdot\text{m}^{-2}$ (15.3%). Figure 10b illustrates the scatterplot of estimated against measured CCC using the CI_{green} . Results for CI_{green} were better than for $CI_{red-edge}$. For this potato experiment the Sentinel-2 band at 705 nm showed no clear decrease or increase with varying the LAI and/or the LCC. Such a feature in the red-edge region is caused by the equal effect of chlorophyll absorption, on the one hand, and canopy scattering, on the other hand [22]. Gitelson et al. [19] found such an equilibrium point at 730 nm when combining data on maize and soybean crops. For potato crops this equilibrium occurs close to 705 nm. As a result, at 705 nm small variations in reflectances between the dates can have a strong influence on a ratio with this band in the denominator, which might explain the larger scatter in the graphs for the $CI_{red-edge}$ (Figure 9).

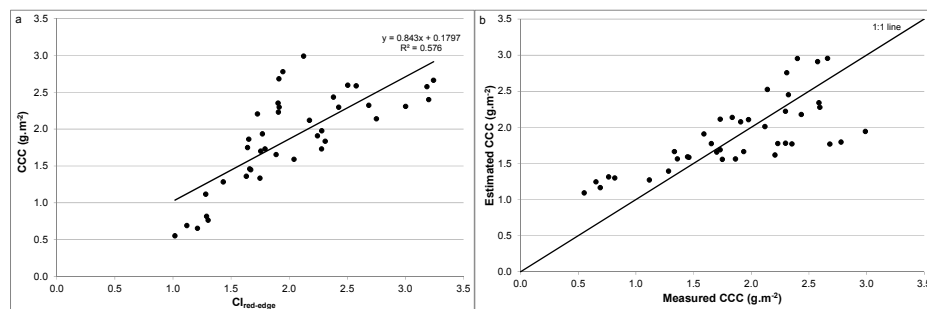


Figure 9. The relationship between the $CI_{red-edge}$ and the CCC (a) and between measured and estimated CCC (b) for the ten plots of the potato experiment on four dates in 2016 using Sentinel-2 data at 20 m resolution.

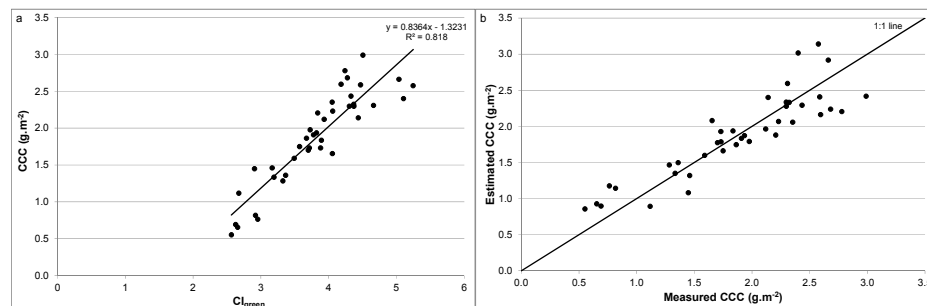


Figure 10. The relationship between the CI_{green} and the CCC (a) and between measured and estimated CCC (b) for the ten plots of the potato experiment on four dates in 2016 using Sentinel-2 data at 10 m resolution.

3.5. Spatial Patterns

Finally, maps of the LAI, LCC, and CCC were created using the Sentinel-2 image of 10 July 2016. This is a date that is still suitable for the farmer to obtain location-specific information of crop N status in order to apply side dressing. Crop development on 7 June 2016 did not yet show large fertilization effects on LAI (Figure 3). Unfortunately, the gap in time between the two Sentinel-2 recordings of 7 June and 10 July was very large for operational applications and should be filled by more satellites (like Sentinel-2B, launched 7 March 2017). Differences in LAI on 10 July, for instance, were very pronounced and, therefore, this date was used for illustration. Figure 11a shows an LAI map obtained from 10 m Sentinel-2 pixels using the relationship shown in Figure 6a. Similarly, Figure 11b shows an LCC map obtained from 10 m Sentinel-2 pixels using the relationship shown in Figures 8a and 11c shows the CCC map using the relationship of Figure 10a.

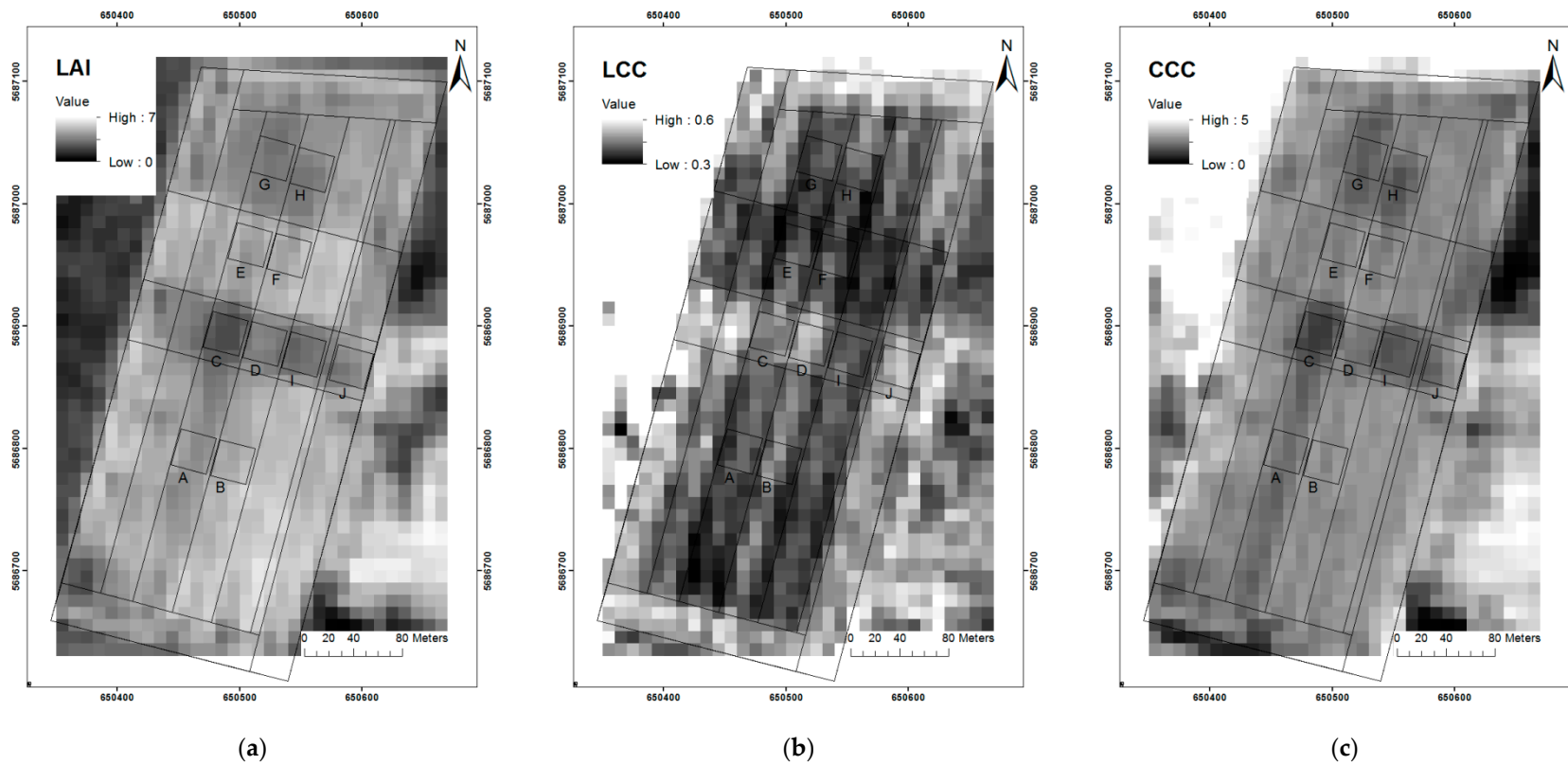


Figure 11. Crop variable maps obtained by applying the obtained statistical relationships to the Sentinel-2 image of 10 July 2016. (a) The LAI map using the WDV_I-LAI relationship of Figure 6a; (b) the LCC map using the CVI-LCC relationship of Figure 8a; and (c) the CCC map using the CI_{green}-CCC relationship of Figure 10a. The overlay shows the location of the net plots (Table 1) and the fertilization zones. The coordinate system is UTM Zone N31 with datum WGS84.

The zone that did not receive any initial fertilization (covering plots C, D, I, and J) is clearly visible in Figure 11a,c, showing relatively low values in the LAI and CCC, as can be expected for the lowest fertilization level. Within this zone plots D and J have higher values than plots C and I due to a large fertilization boost on 28 June 2016 (Table 1). Additionally, the zone with the second-lowest initial fertilization level (covering plots G and H) shows lower LAI and CCC values in Figure 11. Within the next fertilization level covering plots A and B, plot A looks darker, meaning having a lower LAI and CCC value than plot B, because plot B also received additional fertilization on 28 June 2016 (Table 1). Looking at the LCC map (Figure 11b) differences between most plots were not very pronounced, as was already stated in studying the temporal profiles of the TCARI/OSAVI and CVI indices (Figure 4). Plots D and J, without initial fertilization but with a boost of N on 28 June 2016, show the highest LCC values of all ten plots studied. These high LCC values can be explained by the lower LAI values for these plots, meaning that decreased biomass growth caused higher chlorophyll contents in the leaves in this case.

4. Conclusions

This paper presents a proof of concept of using Sentinel-2 satellite data in estimating the LAI, LCC, and CCC in order to support potato crop status assessment for precision agriculture applications. The WDVI is a simple vegetation index that can be estimated using Sentinel-2 10 m bands at 665 nm and 842 nm, assuming the slope of the soil line for these bands is known or determined for bare soil areas in the test area. The WDVI showed good predictive power for estimating LAI for a spatial resolution of 10 m. For estimating the LCC the TCARI/OSAVI ratio showed good results for Sentinel-2. Since this index requires the red-edge bands of Sentinel-2, the LCC is estimated at 20 m spatial resolution. As an alternative, the CVI might be useful. Our results show that the CVI is slightly worse than the TCARI/OSAVI in estimating the LCC. Since the CVI is available at 10 m resolution, it is worthwhile to study further improvements on the atmospheric correction procedure to see whether the CVI might yield better results for Sentinel-2 in the future. Finally, both the $CI_{\text{red-edge}}$ and CI_{green} were tested for estimating the CCC. This study yielded the best results for the CI_{green} . Moreover, this index can be calculated at 10 m spatial resolution, thus estimating the CCC also at this resolution. Results for $CI_{\text{red-edge}}$ were poorer in this study because the equilibrium of effects by chlorophyll absorption and canopy scattering seemed to occur at about 705 nm for potatoes.

Until now many studies have explored the potential of Sentinel-2 based on simulated datasets. At this moment few papers using real Sentinel-2 images for agricultural applications have been published. Immitzer et al. [23] confirmed the expected capabilities for producing reliable land cover maps in Central Europe at 10 m spatial resolution using pre-operational (August 2015) single date Sentinel-2 data. Al-Gaadi et al. [24] used a single date Sentinel-2 image of early 2016 for potato yield prediction in irrigated fields in Saudi Arabia using an empirical relationship with vegetation indices. To our knowledge this is the first paper deriving agricultural crop variables from multi-date Sentinel-2 images.

For operational applications in precision agriculture the 10 m spatial resolution products of Sentinel-2 are already very useful. The temporal resolution should, preferably, be less than one week. Using only Sentinel-2A, the temporal resolution was not yet sufficient for real applications at the individual farmer's level, although our test site was already covered by two orbits. With the additional availability of data from Sentinel-2B (launched 7 March 2017) the temporal resolution will theoretically double, but the number of useful Sentinel-2 images in Western Europe will mainly depend on cloud cover conditions during the critical periods of the growing season.

Acknowledgments: The authors would like to thank Jacob van den Borne for realizing the experimental field, helping with logistics, and supporting the field measurements. Thanks also to Ramin Heidarian Dehkordi for running the SEN2COR atmospheric correction procedure.

Author Contributions: L.K. and M.B. conceived and designed the experiments; M.B. performed the field measurements; J.C. analyzed the data; and J.C. and L.K. wrote the paper.

Conflicts of Interest: The authors declare no conflict of interest.

References

- Houborg, R.; Fisher, J.B.; Skidmore, A.K. Advances in remote sensing of vegetation function and traits. *Int. J. Appl. Earth Obs. Geoinf.* **2015**, *43*, 1–6. [[CrossRef](#)]
- Van Evert, F.K.; Booiij, R.; Jukema, J.N.; ten Berge, H.F.M.; Uenk, D.; Meurs, E.J.J.B.; van Geel, W.C.A.; Wijnholds, K.H.; Slabbekoorn, J.J.H. Using crop reflectance to determine sidedress N rate in potato saves N and maintains yield. *Eur. J. Agron.* **2012**, *43*, 58–67. [[CrossRef](#)]
- Elarab, M.; Ticlavilca, A.M.; Torres-Rua, A.F.; Maslova, I.; McKee, M. Estimating chlorophyll with thermal and broadband multispectral high resolution imagery from an unmanned aerial system using relevance vector machines for precision agriculture. *Int. J. Appl. Earth Obs. Geoinf.* **2015**, *43*, 32–42. [[CrossRef](#)]
- Mulla, D.J. Twenty five years of remote sensing in precision agriculture: Key advances and remaining knowledge gaps. *Biosyst. Eng.* **2013**, *114*, 358–371. [[CrossRef](#)]
- Daughtry, C.S.T.; Walthall, C.L.; Kim, M.S.; de Colstoun, E.B.; McMurtrey, J.E., III. Estimating corn leaf chlorophyll concentration from leaf and canopy reflectance. *Remote Sens. Environ.* **2000**, *74*, 229–239. [[CrossRef](#)]
- Clevers, J.G.P.W.; Kooistra, L. Using hyperspectral remote sensing data for retrieving canopy chlorophyll and nitrogen content. *IEEE J. Sel. Top. Appl. Earth Obs. Remote Sens.* **2012**, *5*, 574–583. [[CrossRef](#)]
- Clevers, J.G.P.W. The application of a weighted infrared-red vegetation index for estimating leaf area index by correcting for soil moisture. *Remote Sens. Environ.* **1989**, *29*, 25–37. [[CrossRef](#)]
- Bouman, B.A.M.; Van Kasteren, H.W.J.; Uenk, D. Standard relations to estimate ground cover and LAI of agricultural crops from reflectance measurements. *Eur. J. Agron.* **1992**, *1*, 249–262. [[CrossRef](#)]
- Kooistra, L.; Clevers, J.G.P.W. Estimating potato leaf chlorophyll content using ratio vegetation indices. *Remote Sens. Lett.* **2016**, *7*, 611–620. [[CrossRef](#)]
- Haboudane, D.; Miller, J.R.; Tremblay, N.; Zarco-Tejada, P.J.; Dextraze, L. Integrated narrow-band vegetation indices for prediction of crop chlorophyll content for application to precision agriculture. *Remote Sens. Environ.* **2002**, *81*, 416–426. [[CrossRef](#)]
- Vincini, M.; Frazzi, E.; D'Alessio, P. A broad-band leaf chlorophyll vegetation index at the canopy scale. *Precis. Agric.* **2008**, *9*, 303–319. [[CrossRef](#)]
- Gitelson, A.A.; Gritz, Y.; Merzlyak, M.N. Relationships between leaf chlorophyll content and spectral reflectance and algorithms for non-destructive chlorophyll assessment in higher plant leaves. *J. Plant Physiol.* **2003**, *160*, 271–282. [[CrossRef](#)] [[PubMed](#)]
- Clevers, J.G.P.W.; Gitelson, A.A. Remote estimation of crop and grass chlorophyll and nitrogen content using red-edge bands on sentinel-2 and -3. *Int. J. Appl. Earth Obs. Geoinf.* **2013**, *23*, 344–351. [[CrossRef](#)]
- Stoorvogel, J.J.; Kooistra, L.; Bouma, J. Managing soil variability at different spatial scales as a basis for precision agriculture. In *Soil-Specific Farming: Precision Agriculture*; Lal, R., Stewart, B.A., Eds.; CRC Press: Boca Raton, FL, USA, 2016; pp. 37–72.
- Uddling, J.; Gelang-Alfredsson, J.; Piikki, K.; Pleijel, H. Evaluating the relationship between leaf chlorophyll concentration and SPAD-502 chlorophyll meter readings. *Photosynth. Res.* **2007**, *91*, 37–46. [[CrossRef](#)] [[PubMed](#)]
- Drusch, M.; Del Bello, U.; Carlier, S.; Colin, O.; Fernandez, V.; Gascon, F.; Hoersch, B.; Isola, C.; Laberinti, P.; Martimort, P.; et al. Sentinel-2: ESA's optical high-resolution mission for GMES operational services. *Remote Sens. Environ.* **2012**, *120*, 25–36. [[CrossRef](#)]
- Delegido, J.; Verrelst, J.; Alonso, L.; Moreno, J. Evaluation of sentinel-2 red-edge bands for empirical estimation of green LAI and chlorophyll content. *Sensors* **2011**, *11*, 7063–7081. [[CrossRef](#)] [[PubMed](#)]
- Dash, J.; Curran, P.J. The MERIS terrestrial chlorophyll index. *Int. J. Remote Sens.* **2004**, *25*, 5403–5413. [[CrossRef](#)]
- Gitelson, A.A.; Viña, A.; Ciganda, V.; Rundquist, D.C.; Arkebauer, T.J. Remote estimation of canopy chlorophyll content in crops. *Geophys. Res. Lett.* **2005**, *32*, L08403. [[CrossRef](#)]
- Louis, J.; Debaecker, V.; Pflug, B.; Main-Knorn, M.; Bieniarz, J.; Mueller-Wilm, U.; Cadau, E.; Gascon, F. *Sentinel-2 SEN2COR: L2A Processor for Users*; (Special Publication) ESA SP-740; European Space Agency: Prague, Czech Republic, 2016.

21. Richter, R.; Schläpfer, D. Geo-atmospheric processing of airborne imaging spectrometry data. Part 2: Atmospheric/topographic correction. *Int. J. Remote Sens.* **2002**, *23*, 2631–2649. [[CrossRef](#)]
22. Gitelson, A.A.; Merzlyak, M.N. Signature analysis of leaf reflectance spectra: Algorithm development for remote sensing of chlorophyll. *J. Plant Physiol.* **1996**, *148*, 494–500. [[CrossRef](#)]
23. Immitzer, M.; Vuolo, F.; Atzberger, C. First experience with Sentinel-2 data for crop and tree species classifications in central Europe. *Remote Sens.* **2016**, *8*, 166. [[CrossRef](#)]
24. Al-Gaadi, K.A.; Hassaballa, A.A.; Tola, E.; Kayad, A.G.; Madugundu, R.; Alblewi, B.; Assiri, F. Prediction of potato crop yield using precision agriculture techniques. *PLoS ONE* **2016**, *11*, e0162219. [[CrossRef](#)] [[PubMed](#)]



© 2017 by the authors. Licensee MDPI, Basel, Switzerland. This article is an open access article distributed under the terms and conditions of the Creative Commons Attribution (CC BY) license (<http://creativecommons.org/licenses/by/4.0/>).